AGU PUBLICATIONS

Water Resources Research

RESEARCH ARTICLE

10.1002/2014WR016553

# A regional estimate of postfire streamflow change in California

Ryan R. Bart[1]

[1]Earth Research Institute, University of California, Santa Barbara, Santa Barbara, California, USA

**Key Points:**

- Regional effect of fire on annual streamflow was estimated using a mixed model
- Annual streamflow in California increased following fire at regional scale
- Postfire streamflow change was sensitive to postfire wetness conditions

**Supporting Information:**

- Supporting Information S1
- Data Set S1

**Correspondence to:**
R. R. Bart,
ryanrbart@eri.ucsb.edu

**Citation:**
Bart, R. R. (2016), A regional estimate of postfire streamflow change in California, *Water Resour. Res.*, *52*, 1465–1478, doi:10.1002/2014WR016553.

Received 14 OCT 2014
Accepted 5 FEB 2016
Accepted article online 8 FEB 2016
Published online 28 FEB 2016



**Abstract** The effect of fire on annual streamflow has been examined in numerous watershed studies, with some studies observing postfire increases in streamflow while other have observed no conclusive change. Despite this inherent variability in streamflow response, the management of water resources for flood protection, water supply, water quality, and the environment necessitates an understanding of postfire effects on streamflow at regional scales. In this study, the regional effect of wildfire on annual streamflow was investigated using 12 paired watersheds in central and southern California. A mixed model was used to pool and statistically examine the combined paired-watershed data, with emphasis on the effects of percentage area burned, postfire recovery of vegetation, and postfire wetness conditions on postfire streamflow change. At a regional scale, postfire annual streamflow increased 134% (82%–200%) during the first postfire year assuming 100% area burned and average annual wetness conditions. Postfire response decreased with lower percentages of percentage area burned and during subsequent years as vegetation recovered following fire. Annual streamflow response to fire was found to be sensitive to annual wetness conditions, with postfire response being smallest during dry years, greatest during wet years, and slowly decreasing during very wet years. These findings provide watershed managers with a first-order estimate for predicting postfire streamflow response in both gauged and ungauged watersheds.

## 1. Introduction

In Mediterranean-Climate Regions (MCRs) such as California, fire is an episodic form of land-cover change whose frequency and severity has increased over the past century due to the influence of humans [*Keeley and Fotheringham*, 2003] and may increase further with climate change [*Williams et al.*, 2001; *Lenihan et al.*, 2003; *Westerling and Bryant*, 2008]. Fire removes above ground vegetation cover and frequently produces hydrophobic soils; initiating a complex recovery sequence where hydrophobicity breaks down with successive rainfall events and burned shrubland stands become reestablished after crowding out opportunistic herbaceous vegetation [*Keeley and Keeley*, 1981; *Shakesby and Doerr*, 2006].

Fire has been observed to impact many aspects of the streamflow regime, including peak flow, base flow, and water yield [*Keller et al.*, 1997; *McMichael and Hope*, 2007; *Kinoshita and Hogue*, 2011]. While there is a basic understanding of the individual hydrologic processes affected by fire (e.g., interception, soil infiltration, and transpiration), predicting how streamflow may respond to fire for a given watershed remains challenging since the effect of these processes on streamflow varies spatially from watershed to watershed and temporally as watershed conditions undergo a postfire recovery sequence. Spatial and temporal variability stems from the uniqueness of watershed physiographic properties, meteorological conditions, and vegetation types; the extent, location, and severity of the fire; and the postfire recovery rate of vegetation and soils. Consequently, postfire streamflow responses are largely representative of the specific watershed and conditions that produced the response.

Streamflow response to fire in MCR watersheds varies widely across watersheds, with many empirical studies observing postfire increases in streamflow [*Hoyt and Troxell*, 1932; *Lavabre et al.*, 1993; *Scott*, 1993; *Loáiciga et al.*, 2001; *Jung et al.*, 2009], while others have observed no conclusive change in streamflow [*Britton*, 1991; *Aronica et al.*, 2002; *Bart and Hope*, 2010] or streamflow decreases [*Nolan et al.*, 2015]. Despite this inherent variability in streamflow response, the management of water resources for flood protection, water supply, water quality, and the environment necessitates an understanding of postfire effects on streamflow at a regional scale. This knowledge is essential for prediction in both gauged and ungauged watersheds.

Despite numerous investigations into the effect of fire on annual streamflow at the watershed scale, a regional estimate of postfire streamflow response for central and southern California has not been established. Some reviews on the general effects of vegetation change on streamflow have included, but do not exclusively pertain to fire [*Bosch and Hewlett*, 1982; *Brown et al*., 2005]. On the other hand, recent reviews by *Moody and Martin* [2009] and *Smith et al*. [2011] have investigated the effects of fire on sediment and water quality, respectively, but no known studies have examined the regional effect on postfire annual streamflow.

The research objective of this study was to combine streamflow data from 12 paired-watershed studies in California in order to investigate the regional effect of fire on annual streamflow. The paired-watershed technique entailed pairing streamflow from each burned watershed with streamflow from an unburned watershed to act as a control. A mixed model was then used to pool and statistically examine the combined data. Pooling data from multiple watersheds, as opposed to examining a single watershed as is typically done in paired-watershed analyses, enabled this study to examine the effect of percentage area burned, the postfire recovery of vegetation, and postfire wetness conditions on streamflow following fire.

Some of the watersheds included in this study have previously been analyzed on an individual basis to test for the effect of fire on streamflow [*Hoyt and Troxell*, 1932; *Bart and Hope*, 2010; *Kinoshita and Hogue*, 2011]. *Hoyt and Troxell* [1932] conducted one of the earliest paired-watershed studies using data from Fish Creek following a fire in 1924. This study reported a 29% increase in postfire water yield and an increase in both peak flow rates and base flow levels. *Kinoshita and Hogue* [2011] conducted a study of City Creek and Devil Canyon Creek following a large fire in 2003 and noted that both water yield and dry season base flow increased throughout the postfire period. *Bart and Hope* [2010] investigated the effect of fire on postfire streamflow in six large ($>$50 km$^2$) central California watersheds using the paired-watershed technique. Few instances of statistically significant postfire streamflow change were reported by these authors, with most postfire streamflow falling within the uncertainty of the prefire calibrated model. However, *Bart and Hope* [2010] did note that the few instances of statistically significant postfire streamflow change were associated with years of normal or above-normal annual streamflow. A similar relation between postfire streamflow change and annual wetness conditions has also been observed by *Feikema et al*. [2013] for Australian watersheds.

## 2. Watershed Selection and Data

The watersheds in this study were selected from U.S. Geological Survey (USGS) streamflow gauges in central and southern California. Watersheds were evaluated for inclusion based on the absence of major diversions or regulations, lack of persistent winter snow cover, little urbanization or agriculture, and data record. Fire history for each watershed was obtained from the Fire and Resource Assessment Program (FRAP) (http://frap.fire.ca.gov). Paired watersheds were selected by first identifying watersheds that had a fire that burned at least 20% of the watershed area and had no additional fires greater than 5% of the watershed area during the prefire and postfire periods. All watersheds in the vicinity of the candidate burned watersheds were then evaluated for also having no fires greater than 5% of the watershed area during the combined prefire and postfire period to act as a control watershed.

A total of 12 burned watersheds and 8 control watersheds were identified for inclusion in the study (Table 1). All burned watersheds met the selection criteria outlined above except San Antonio, Santa Paula, and City which had fires during the prefire period of 7%, 16%, and 6% of area burned, respectively. The study watersheds are located along the Coast Range of central California and the Transverse Range of southern California (Figure 1). The area encompassing these watersheds is characterized by a Mediterranean climate regime, with hot dry summer and mild wet winters. Most rainfall is generated by cyclonic frontal systems approaching from the Pacific Ocean. Since the mountains of the Coast and Transverse Ranges are topographically very steep, orographic effects drive precipitation totals during the wet season.

Watershed characteristics were obtained from the Geospatial Attributes of Gages for Evaluating Streamflow (GAGES-II) database assembled by *Falcone* [2011] (Table 1). The burned watersheds had areas ranging from 7 km$^2$ to over 600 km$^2$, with the smaller watersheds concentrated in the southern portion of the region. Annual precipitation totals varied from 385 to 1163 mm/yr, while mean annual streamflow ranged from 22 to 753 mm/yr. The lithology of the watersheds in the Transverse Range is dominated by igneous and

**Table 1.** Watershed Characteristics

| # | Watershed Name | USGS ID | Area (km$^2$) | Mean Annual Precipitation (mm) | Mean Annual PET (mm) | Mean Annual Streamflow (mm) | Dominant Geology Type | Stream Density (km/Km$^2$) | Mean Slope (%) | Mean Soil Depth (mm) | Mean Clay Percentage | Mean Silt Percentage | Shrubland Percentage |
|---|---|---|---|---|---|---|---|---|---|---|---|---|---|
| 1 | City Creek | 11055801 | 50.5 | 781 | 729 | 226 | Quarternary | 1.21 | 34.4 | 650 | 13.2 | 30.6 | 77.5 |
| 2 | Devil Canyon Creek | 11063680 | 14.4 | 940 | 762 | 165 | Quarternary | 1.45 | 39.0 | 492 | 14.5 | 32.1 | 76.7 |
| 3 | Day Creek | 11067000 | 12.0 | 1155 | 648 | 309 | Gneiss | 0.92 | 50.9 | 518 | 14.1 | 32.1 | 48.3 |
| 4 | Fish Creek | 11084500 | 15.4 | 841 | 772 | 271 | Gneiss | 1.26 | 39.2 | 493 | 16.5 | 45.7 | 70.8 |
| 5 | Little Dalton Creek | 11086500 | 7.2 | 734 | 804 | 92 | Gneiss | 0.77 | 35.9 | 456 | 18.2 | 49.7 | 87.1 |
| 6 | Arroyo Seco (South) | 11098000 | 41.6 | 788 | 776 | 215 | Granitic | 1.13 | 42.8 | 461 | 17.7 | 48.2 | 70.9 |
| 7 | Santa Anita Creek | 11100000 | 25.0 | 969 | 762 | 239 | Granitic | 1.01 | 44.1 | 475 | 17.3 | 47.6 | 46.6 |
| 8 | Sespe Creek | 11111500 | 128.5 | 850 | 552 | 120 | Sedimentary | 1.25 | 26.5 | 573 | 22.1 | 41.3 | 45.9 |
| 9 | Santa Paula Creek | 11113500 | 103.3 | 678 | 709 | 220 | Sedimentary | 1.18 | 34.4 | 621 | 23.6 | 44.2 | 55.6 |
| 10 | Coyote Creek | 11117600 | 33.9 | 729 | 736 | 216 | Sedimentary | 1.10 | 31.2 | 603 | 25.9 | 44.7 | 46.8 |
| 11 | Carpinteria Creek | 11119500 | 34.1 | 710 | 725 | 107 | Sedimentary | 1.06 | 32.6 | 643 | 23.8 | 44.7 | 36.3 |
| 12 | Santa Cruz Creek | 11124500 | 191.5 | 831 | 637 | 96 | Sedimentary | 1.17 | 33.5 | 646 | 23.9 | 41.1 | 47.3 |
| 13 | Lopez Creek | 11141280 | 54.0 | 717 | 741 | 170 | Sedimentary | 0.69 | 37.1 | 658 | 32.6 | 38.8 | 27.8 |
| 14 | Arroyo De La Cruz | 11142500 | 106.8 | 906 | 716 | 460 | Sedimentary | 0.92 | 28.1 | 714 | 34.3 | 40.4 | 26.3 |
| 15 | Big Sur River | 11143000 | 120.6 | 1163 | 640 | 753 | Granitic | 0.98 | 43.6 | 633 | 14.1 | 31.5 | 33.1 |
| 16 | Nacimiento River | 11148900 | 403.5 | 692 | 745 | 409 | Sedimentary | 0.99 | 21.3 | 720 | 22.9 | 36.9 | 40.8 |
| 17 | San Antonio River | 11149900 | 556.4 | 633 | 737 | 174 | Sedimentary | 1.13 | 19.5 | 862 | 24.4 | 37.8 | 39.1 |
| 18 | Arroyo Seco (North) | 11152000 | 625.1 | 809 | 664 | 243 | Sedimentary | 1.03 | 34.7 | 644 | 20.2 | 34.8 | 42.2 |
| 19 | Los Gatos Creek | 11224500 | 247.4 | 470 | 792 | 22 | Sedimentary | 1.19 | 26.1 | 857 | 35.6 | 40.3 | 67.7 |
| 20 | Cantua Creek | 11253310 | 120.4 | 385 | 823 | 25 | Sedimentary | 1.24 | 24.3 | 947 | 36.6 | 36.7 | 42.5 |

metamorphic rocks while the watersheds in the Coast Range are primarily composed of sedimentary rocks. Soils are relatively shallow (456–947mm), particularly in the steeper watersheds. Chaparral shrublands are the dominant vegetation in many of the watersheds, although grasslands, coastal sage scrub, oak woodlands, and forests are also common [*Callaway and Davis*, 1993].

Each burned watershed and its corresponding control watershed is listed in Table 2. The percentage of watershed area burned ranged from 23% to 100% across all the watersheds, with higher percentages more commonly observed in smaller watersheds. Some of the control watersheds were located nearly 100 km

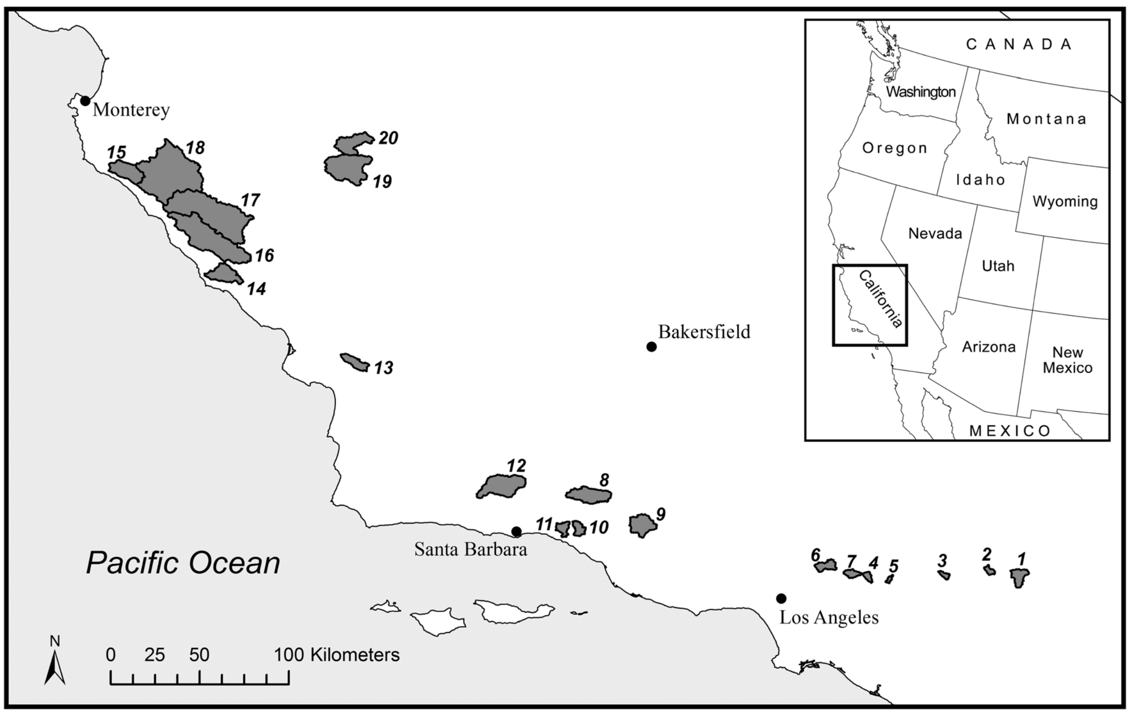


**Figure 1.** Location of selected research watersheds in California. Number corresponds to name and description in Table 1.

**Table 2.** Summary of Paired Watershed and Fire Characteristics[a]

| Burnt Watershed | Fire Year | Area Burned (%) | Control Watershed | Distance Between Pairs (km) | Prefire Period | Postfire Period | $R^2$ |
|---|---|---|---|---|---|---|---|
| Arroyo Seco (N) | 1977 | 63 | San Antonio | 29 | 1966–1977 | 1978–1984 | 0.98 |
| Big Sur | 1977 | 92 | Arroyo de la Cruz | 72 | 1966–1977 | 1978–1979 | 0.93 |
| Cantua | 1979 | 23 | Los Gatos | 14 | 1967–1979 | 1980–1986 | 0.89 |
| Carpinteria | 1971 | 84 | Coyote | 8 | 1959–1971 | 1972–1977 | 0.96 |
| City | 2003 | 94 | Arroyo Seco (S) | 89 | 1985–2003 | 2004–2010 | 0.85 |
| Devil Canyon | 2003 | 97 | Arroyo Seco (S) | 75 | 1985–2003 | 2004–2010 | 0.69 |
| Fish | 1924 | 100 | Santa Anita | 9 | 1918–1924 | 1925–1931 | 0.96 |
| Little Dalton | 1960 | 100 | Day | 27 | 1940–1960 | 1961–1967 | 0.92 |
| Lopez | 1985 | 100 | Santa Cruz | 97 | 1968–1985 | 1986–1992 | 0.89 |
| San Antonio | 1985 | 31 | Nacimiento | 14 | 1972–1985 | 1986–1992 | 0.95 |
| Santa Paula | 1985 | 71 | Santa Cruz | 68 | 1960–1985 | 1986–1992 | 0.90 |
| Sespe | 1985 | 40 | Santa Cruz | 41 | 1960–1985 | 1986–1992 | 0.79 |

[a]$R^2$ corresponds to the relation between prefire annual streamflow ($\log_e$) in the burned and control watersheds.

from the burned watershed. While differences in precipitation and watershed characteristics between the burned and control watersheds may be expected to increase with distance between watershed pairs, *Bart and Hope* [2010] observed that the correlation of annual streamflow for paired watersheds at this distance was suitable for postfire streamflow change analysis in California. For this study, 10 out of the 12 watershed pairs had $R^2$ values greater than 0.85 for prefire annual streamflow ($\log_e$) between the control and burned watersheds, with the lowest being 0.69 for Devil Canyon and its control Arroyo Seco (Table 2). The average length of the prefire period was 16.6 years, ranging from 7 to 26 years. The postfire period was monitored for up to 7 years.

## 3. Methodology

### 3.1. Mixed Model

Annual streamflow data from 12 paired-watershed experiments were pooled into a single data set to statistically evaluate regional changes in postfire streamflow. The relation between annual streamflow for each burned and control watershed differed by watershed pair. This was due to the data set containing a hierarchical structure, with streamflow values for the lower, streamflow level of the hierarchy being dependent on the higher, group or watershed level of the hierarchy from which the streamflow values were selected. The lower level of this hierarchy is referred to as level 1 and hereby denoted with an *i* subscript, while the higher level is referred to as level 2 and denoted with a *j* subscript. Mixed modeling is a statistical approach that is similar to regression analysis but can account for hierarchies within data by partitioning model error to each level of the hierarchy using variables containing random effects [*Bickel*, 2007]. Mixed modeling is referred to by many different names in the literature; multilevel modeling, hierarchical modeling, generalized linear mixed modeling (GLMM), mixed-effect modeling, and meta-analysis; and has recently been used for an increasing number of hydrologic applications [*Clarke*, 2001; *Lopez-Moreno and Stähli*, 2008; *Seo et al.*, 2008; *Wehrly et al.*, 2009; *Webb and Kathuria*, 2012; *Chamizo et al.*, 2013; *Lessels and Bishop*, 2013; *Walsh and Webb*, 2014].

A two-level mixed model with no predictor variables (i.e., unconditional model) may be represented as

$$y_{ij} = \beta_0 + u_j + e_{ij} \tag{1}$$

where $y_{ij}$ is the $i$th observation of the dependent variable (i.e., annual streamflow) from the $j$th group (i.e., watershed), $\beta_0$ is the intercept of the model, $u_j$ is the level-2 model error for the $j$th group, and $e_{ij}$ is the level-1 model (residual) error for the $i$th observation from the $j$th group. It is generally assumed that the distribution of the model errors is normal with a mean of 0 and a variance of $\sigma^2$, such that $u_j \sim N(0, \sigma_u^2)$ and $e_{ij} \sim N(0, \sigma_e^2)$. Model error $u_j$ represents the deviation of the level-2 groups from the overall mean, and model error $e_{ij}$ represents the deviation of level-1 data from the corresponding level-2 group mean.

The unconditional model in equation (1) provides a baseline estimate of the variance in the dependent variable. Predictor variables may be introduced to the model in order to reduce this variance. A conditional mixed model with a level-1 predictor variable may be represented by

$$y_{ij}=\beta_0+\beta_1 x_{ij}+u_j+e_{ij} \quad (2)$$

where $x_{ij}$ is the $i$th observation of the level-1 predictor variable for the $j$th group and $\beta_1$ is the model slope.

The model represented by equation (2) is often referred to as a random intercept model because the intercept for each level-2 group varies randomly across groups. The random intercept model assumes that the slope of the relation between a predictor variable and the dependent variable is constant across groups. This assumption may not always be appropriate. Random slope models are mixed models where the both the intercept and the slope are allowed to vary across watersheds. A random slope model for equation (2) can be written as

$$y_{ij}=\beta_0+\beta_1 x_{ij}+u_{0j}+u_{1j}x_{ij}+e_{ij}. \quad (3)$$

The level-2 random effects are now represented by two terms, $u_{0j}$ for the random intercept and $u_{1j}$ for the random slope. Note that $u_{1j}$ interacts with $x_{ij}$, indicating the slope of the relation between the dependent variable and the predictor variable may vary by group. A second variable is also generated from the random slope model, $\sigma_{u01}$, representing the covariance between $u_{0j}$ and $u_{1j}$.

### 3.2. Model Calibration and Cross Validation

The standard approach for calibrating mixed models is the maximum likelihood method [*Hox*, 2002], which attempts to maximize a likelihood function for optimal model fit. The maximum likelihood method is based on large-sample theory and maximum likelihood estimates and confidence intervals are considered to be very robust when level-2 sample sizes are large [*Hox*, 2002]. However, the method has been shown to be severely biased when the level-2 sample sizes are small [*Stegmueller*, 2013]. For small samples, it is recommended that Bayesian estimation procedures be used instead of maximum likelihood [*Hox*, 2002; *Stegmueller*, 2013]. With Bayesian approaches, a prior probability distribution is developed and combined with an estimate of the likelihood of the data to produce a posterior probability distribution, which represents the uncertainty of the model. Although the posterior distribution is generally too complicated to compute directly, Markov Chain Monte Carlo (MCMC) procedures have been developed to generate random samples from the posterior distribution. These samples, when repeated many times, can provide estimates and confidence intervals for mixed model parameters.

As the level-2 sample size for watersheds in this study was 12, a Bayesian estimation procedure was used to calibrate the model. Mixed modeling methods were carried out with the R programming language (www.r-project.org) using the MCMCglmm [*Hadfield*, 2010] package. An improper, noninformative prior was used to minimize the effect of the prior on the model results, while the likelihood was assumed to have a Gaussian distribution. A Gibbs sampling algorithm was used for the MCMC walk [*Hadfield*, 2010] and 1,000,000 iterations with a thinning of 20 were used to calibrate each model. Model convergence was assessed visually.

The test statistic used for model calibration was the Deviance Information Criterion (DIC) [*Hadfield*, 2010]. The DIC is a generalization of the Akaike information criterion and is defined as

$$DIC=\bar{D}+p_D \quad (4)$$

where $\bar{D}$ is a measure of model fit and $p_D$ is a measure of model complexity. $\bar{D}$ is the average deviance $D$ over all MCMC iterations, with deviance defined as

$$D=-2\ln\left(p(y|\theta)\right) \quad (5)$$

$p(y|\theta)$ is the likelihood function and $\theta$ is a parameter of the model. The variable $p_D$ is a measure of the effective number of parameters [*Spiegelhalter et al*., 2002]. Models with smaller values of DIC indicate better calibrated model fit, however, in some cases, DIC has been found to overfit models [*Plummer*, 2008].

The DIC provides an estimate of the model fit for the dependent variable; annual streamflow in the burned watershed. However, the objective of this study was to investigate the regional effect of fire, an independent variable (see section 4.3), on annual streamflow. To accomplish this latter objective, and to ensure that the model was not overly complex for the available data, leave-one-out cross validation was used to evaluate how well each model predicted annual streamflow response to fire [*Kohavi*, 1995].

The leave-one-out cross-validation technique systematically holds one watershed out of model calibration for use during validation. The model was calibrated on the remaining 11 watersheds and used to predict

**Table 3.** Model Structures Tested for Predicting Annual Streamflow in the Burned Watershed

| Model | Model Components |
|---|---|
| 1 | By-watershed random intercepts |
| 2 | Model 1 + Annual streamflow from the control watershed |
| 3 | Model 2 + By-watershed random slopes for annual streamflow from the control watershed |
| 4a | Model 3 + Fire (Uniform) |
| 4b | Model 3 + Fire (Percentage area burned) |
| 4c | Model 3 + Fire (Postfire recovery) |
| 4d | Model 3 + Fire (Percentage area burned and postfire recovery) |
| 5 | Model $4_{top}$ + Interaction variable (Fire × Annual streamflow from the control watershed) |

the effect of fire for the validation watershed. This process was repeated for each watershed and mean square error (MSE) was computed to compare the modeled postfire streamflow change with the observed postfire streamflow change in the validation watersheds. MSE is defined as

$$MSE=\frac{1}{N}\sum_{i=1}^{p}\sum_{j=1}^{q_i}\left(y_{ij}-\hat{y}_{ij}\right)^2 \tag{6}$$

where $\hat{y}_{ij}$ is the difference between the $j$th mixed-model predicted postfire streamflow value in the $i$th watershed assuming fire and the $j$th mixed-model predicted postfire streamflow value in the $i$th watershed assuming no fire; $y_{ij}$ is the difference between the $j$th observed postfire streamflow value in the $i$th watershed and the $j$th postfire streamflow value in the $i$th watershed predicted from a prefire linear regression model; $p$ is the total number of watersheds; $q_i$ is the number of postfire years in the $i$th watershed; and $N$ is equal to the total number of postfire wateryears for all the watersheds.

### 3.3. Model Development and Model Variables

To test the regional effect of fire on annual streamflow in central and southern California, a mixed model was developed to predict annual streamflow (mm) from the burned watershed. Annual streamflow was observed to be independent from one wateryear (October–September) to the next (lag-1 correlation coefficient ($r$) for annual streamflow in each of 12 burned watersheds ranged from −0.34 to 0.27) since the extended summer dry period in California produces very low soil moisture and storage levels that coincide with end of the wateryear [*Miller et al.*, 1983]. Model development began with a parsimonious base model and proceeded by incrementally adding more complexity to the model (Table 3). The base model included random intercepts for watershed, but no predictor variables (Model 1). Following the addition of each model variable, the value of the DIC calibration statistic and MSE validation statistic (the latter for models including a fire variable) was evaluated to determine if the new variable improved model fit.

Annual streamflow from the control watersheds was expected to be the strongest predictor of annual streamflow from the burned watersheds by controlling for interannual differences in precipitation and hydrologic behavior (Model 2). Since the relation between annual streamflow from the burned and control watersheds was heteroscedastic and nonnormal, streamflow data from both watersheds were transformed ($\log_e$) for all models in the study, including Model 1. In some cases, the log transformation of very small annual streamflow totals (less than 1 mm) produced disproportionately influential points due to the amplification of very small differences in annual streamflow. Influential points with a Cook's distance greater than one [*Ryan*, 1997] were removed following the approach outlined in *Bart and Hope* [2010]. Annual streamflow from the control watersheds was group-mean centered by subtracting the mean of the level-2 group to which each value was associated [*Enders and Tofighi*, 2007].

Model 3 tested whether the addition of by-watershed random slopes for annual streamflow from the control watershed provide a better model fit than the random intercepts of Model 2 (Table 3).

Model 4 incorporated a fire variable for characterizing postfire watershed conditions. As the postfire recovery of watershed conditions is highly variable, there is no established approach for defining postfire watershed conditions in California. Some studies have treated the postfire period as having uniformly burned conditions for a fixed period of time (i.e., dummy variable) [*Loáiciga et al.*, 2001; *Bart and Hope*, 2010]. However, an alternative approach is to include a fire variable that approximates the postfire recovery of watershed conditions. This latter approach is likely to provide a more realistic representation of postfire watershed conditions. Further, since the effect of fire lessens with time, the subjective designation of postfire length becomes less critical than under uniform conditions.

Four fire variables representing different metrics of postfire change and postfire watershed recovery were tested and compared in this study to determine which variable most accurately characterized postfire

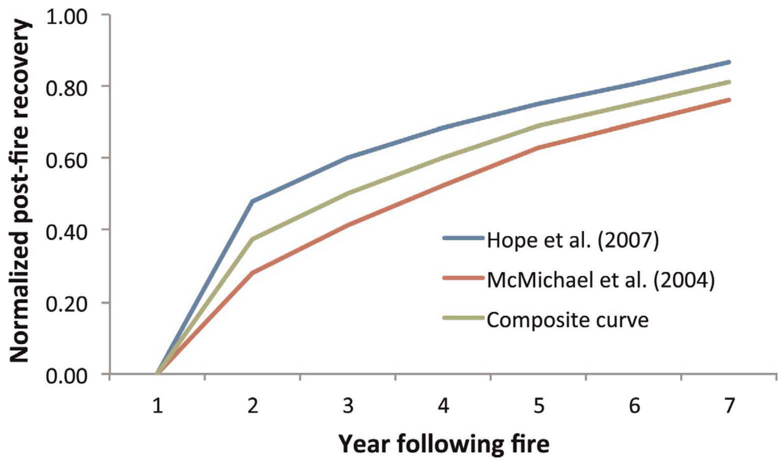


**Figure 2.** Normalized postfire vegetation recovery curve.

watershed conditions. For each of the fire variables, watershed conditions during the prefire period were assumed to be uniform, or unvarying. For the postfire period, the first variable assumed that the initial postfire change was equal for all watersheds and that postfire conditions were uniform throughout a 7 year period following fire (Model 4a). The second fire variable tested accounted for watershed-to-watershed differences in the initial postfire change by weighting the postfire period by the percentage of watershed area burned (Model 4b). While the percentage of area burned does not account for the severity of the fire or spatial differences from burning in hydrologically connected verses unconnected areas, it does provides an estimate of the differences in initial postfire watershed conditions between watersheds. The third variable tested assumed that the initial postfire change was equal for all watersheds but accounted for the temporal recovery of watershed conditions following fire by weighting the postfire period by the reverse scaling (i.e., 1 minus value) of a normalized postfire vegetation recovery curve (see next paragraph) (Model 4c). The postfire period of the fourth fire variable tested was weighted by both the percentage of watershed area burned and the normalized postfire vegetation recovery curve (Model 4d).

The normalized postfire vegetation recovery curve is a single curve used to characterize the postfire recovery for all watersheds in the study and was derived from two remote sensing studies in central California [*McMichael et al.*, 2004; *Hope et al.*, 2007] (Figure 2). This curve was required since some of the fires in the study date from the presatellite era and characterizing the recovery of each burned watershed was not possible. *McMichael et al.* [2004] used a chronosequence technique to develop a postfire recovery curve for shrubland leaf-area index (LAI) while *Hope et al.* [2007] used a NDVI time series to directly produce a recovery curve for shrubland stands. These studies observed that postfire recovery of above ground vegetation ranged from 10 to 15 years following fire. The normalized postfire vegetation recovery curve did not incorporate the postfire recovery of soils since no large-scale estimate of soil recovery was available. As soils may be expected to recover faster than vegetation [*Shakesby and Doerr*, 2006], this omission may cause the model to underestimate postfire streamflow response during years when streamflow is affected by postfire changes in soil hydrophobicity and overestimate postfire streamflow response when streamflow is unaffected. It should also be noted that since the normalized postfire vegetation recovery curve only takes into account shrubland recovery, differences in the postfire recovery of other vegetation types within the watershed might add uncertainty to the model results.

Model 5 examined how postfire streamflow response varies with interannual (level 1) changes in watershed conditions. Model 5 added a level-1 interaction variable to the top-performing Model 4 (herein referred to as Model $4_{top}$) in order to investigate how the effect of fire varies from wateryear to wateryear with changes in annual wetness conditions (Table 3). The interaction variable was generated from the product of the two interacting variables; the fire variable introduced in Model $4_{top}$ and annual streamflow from the control watershed. The magnitude of annual streamflow from the control watershed was assumed to be representative of annual wetness conditions.

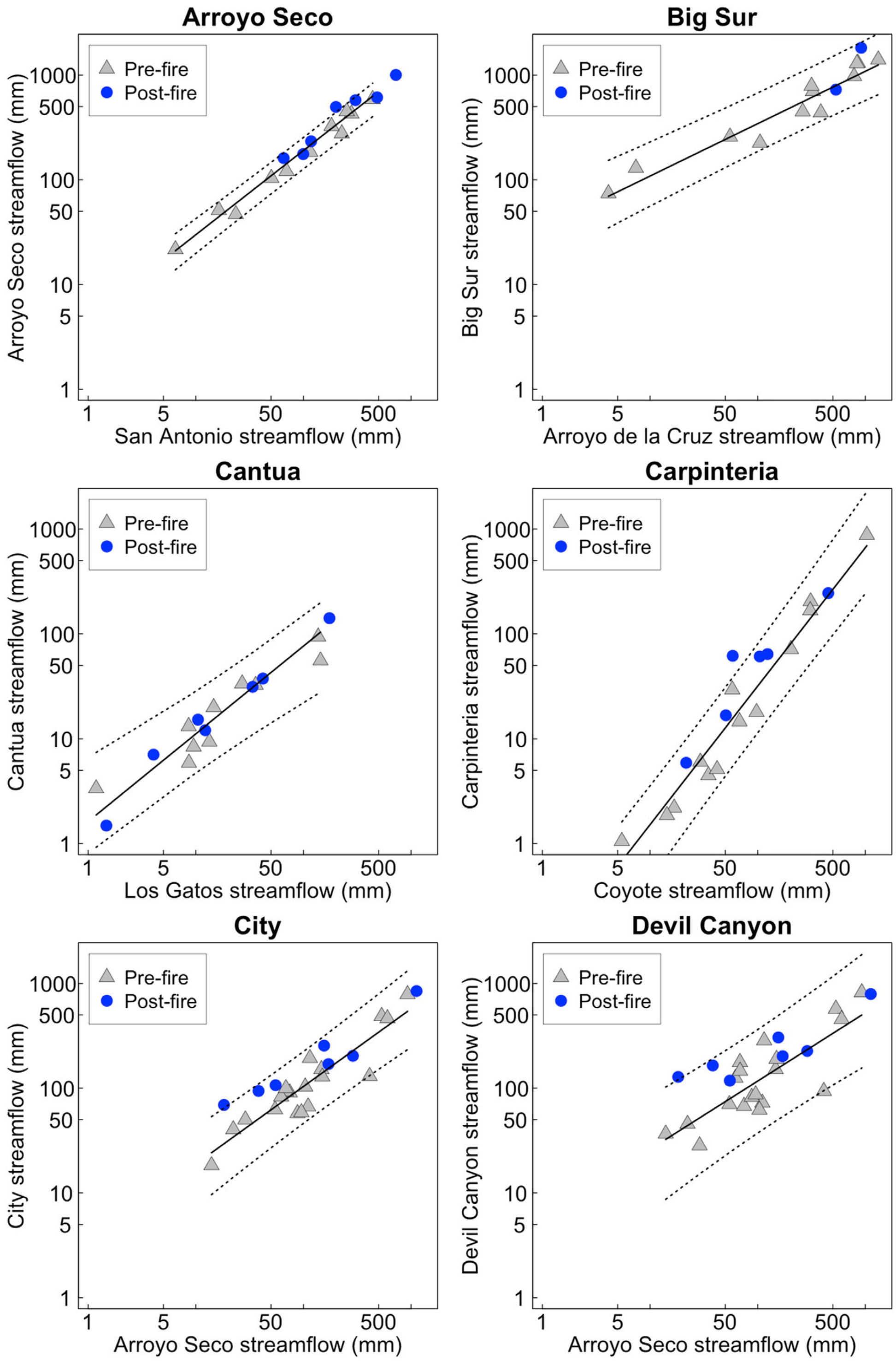


**Figure 3.** Annual streamflow from the burned watershed (*y* axis) plotted against annual streamflow from the control watershed (*x* axis). Solid black line represents linear regression model fitted to prefire annual streamflow. Dashed black lines represent prediction intervals for prefire relation.

## 4. Results

Plots of prefire and postfire annual streamflow totals for each of the burned and control watersheds are displayed in Figure 3. A linear least squares regression model (solid line) with corresponding prediction intervals (dashed lines) was fitted to the prefire streamflow of each watershed pair. Linear regression represents

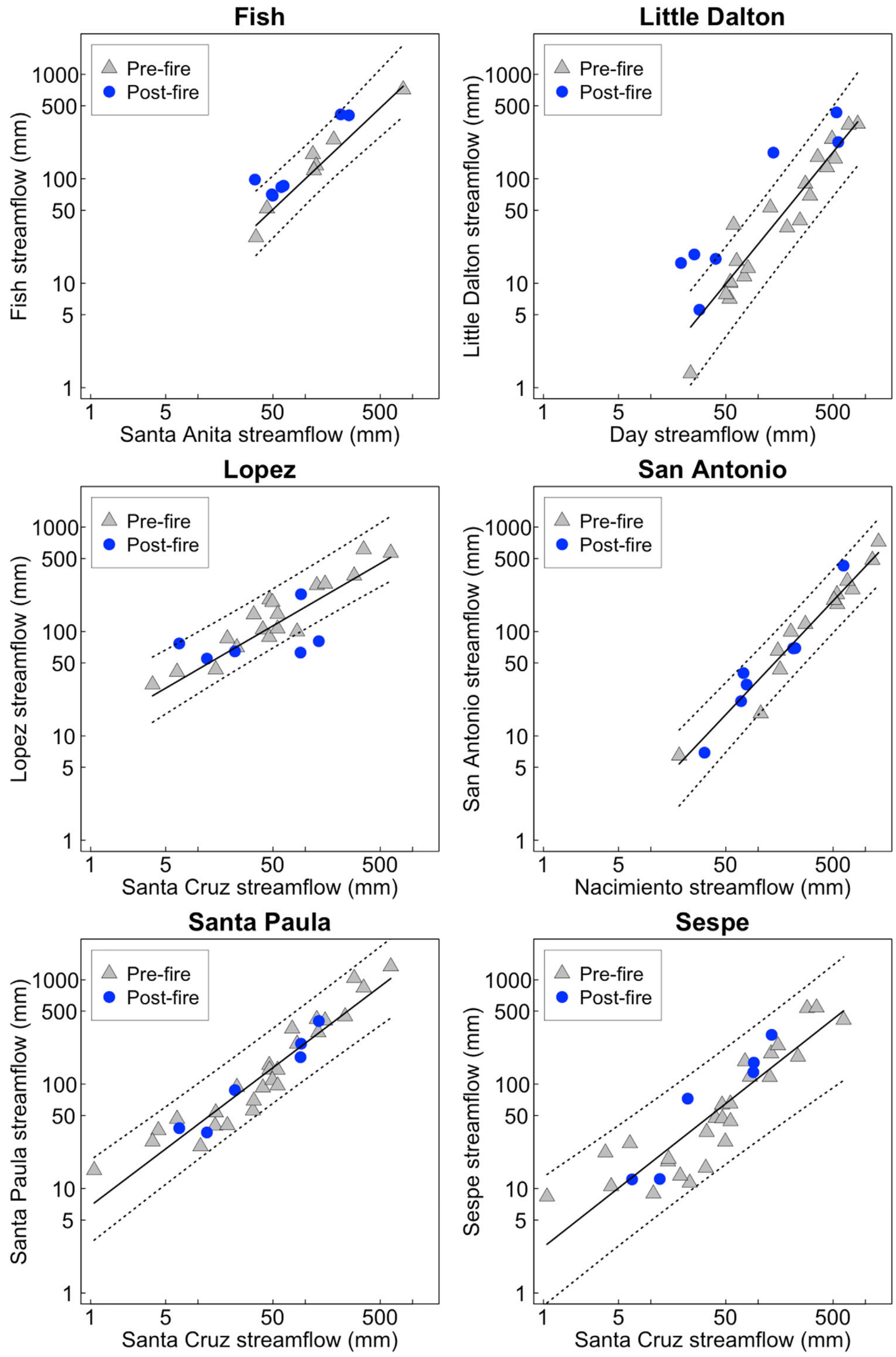


**Figure 3.** (continued)

the standard approach for modeling individual paired-watershed relations. For many of the burned watersheds (e.g., Big Sur, Cantua, San Antonio, Santa Paula, and Sespe), the deviations of the postfire annual streamflow data about the regression line did not exceed the variability of the prefire data, indicating that postfire change may not be detectable for some paired watersheds on an individual basis [*Bart and Hope*, 2010]. However, examining the results across all 12 watershed pairs, 74.7% of postfire annual streamflow

**Table 4.** Calibration and Validation Statistics for Each of the Tested Models[a]

| Model | Calibration DIC | Validation MSE |
|---|---|---|
| 1 | 873.6 | |
| 2 | 455.5 | |
| 3 | 372.1 | |
| 4a | 348.2 | 1.43 |
| 4b | 344.2 | 1.37 |
| 4c | 335.3 | 1.25 |
| 4d | 328.6 | 1.17 |
| 5 | 323.4 | 1.00 |

[a]DIC is Deviance Information Criterion and MSE is mean squared error.

points plotted above the prefire linear regression lines. This implies that at a regional scale, postfire annual streamflow may have increased in the burned watersheds relative to the control watersheds.

Table 4 presents the calibration and validation statistics generated during the development of each mixed model. The mode and 95% credible (i.e., confidence) intervals for each fixed and random model parameter are displayed in Tables 5 and 6, respectively.

The base model consisting of a random intercept model grouped by watershed with no predictor variables is shown as Model 1. The addition of annual streamflow from the control watersheds as a predictor variable (Model 2) and the inclusion of random slopes between annual streamflow from the burned and control watersheds (Model 3) improved calibration fit relative to Model 1, with DIC decreasing from 873.6 to 372.1 (Table 4). For the base model, the only fixed effect calculated was the intercept, which represents the population mean for logged annual streamflow from the burned watersheds, adjusted for the hierarchical structure of the data. For Models 2 and 3, annual streamflow from the control watershed was a highly significant predictor of annual streamflow in the burned watershed (Table 5), reflecting the strong relation ($R^2$) observed between the two variables (Table 2).

Four different fire predictor variables, uniform conditions (Model 4a), percentage area burned (Model 4b), postfire recovery (Model 4c), and both percentage area burned and postfire recovery (Model 4d), were added individually to Model 3 to test the effect of fire on annual streamflow. Model 4a showed a decrease in DIC to 348.2, a cross-validation MSE value of 1.43, and had a fire coefficient value of 0.31. The antilog of this coefficient value equates to a 36% (20%–53%) increase in annual streamflow for each postfire year and for all fire sizes. Model 4b showed a slightly improved fit (DIC = 344.2, MSE = 1.37) and an increase in postfire annual streamflow of 52% (30%–76%) assuming 100% area burned. For watersheds that are only partially burned, the corresponding postfire streamflow response would be smaller. Model 4c further improved fit with a reduction in DIC to 335.3 and MSE to 1.25. The improved fit of Model 4c relative to Model 4b suggests that accounting for the postfire recovery of watershed conditions is more important than accounting for watershed differences in the percentage of area burned. Postfire annual streamflow in Model 4c increased 86% (54%–132%) during the first postfire wateryear. Model 4d, which accounted for both percentage area burned and the postfire recovery of watershed conditions, provided the best fit (DIC = 328.6, MSE = 1.17) was selected as Model $4_{top}$. Model 4d predicted that the regional effect of fire during the first postfire wateryear for a watershed that is 100% burned would be a 136% (84%–208%) increase in annual streamflow.

For a given percentage of area burned and for a given postfire year, the effect of fire on annual streamflow was assumed to be equal under all conditions for Models 4d. A level-1 interaction variable between the fire variable from Model 4d and antecedent streamflow from the control watershed was included in Model 5 to test whether the effect of fire on annual streamflow varies with annual wetness conditions. Model fit improved with Model 5; DIC decreased to 323.4 and MSE decreased to 1.00 (Table 4). The fire variable in Model 5 predicted that postfire annual streamflow would increase 134% (82%–200%) during the first postfire year assuming 100% area burned (Table 5). This value represented the effect of fire on annual streamflow for average annual wetness conditions for the region, specifically when annual streamflow from the control watershed was at its centered mean value of 76 mm. The interaction variable modified this effect when annual streamflow from the control watershed was above or below the centered value. On a percent change basis, postfire annual streamflow decreased by 19% (3%–32%) for every doubling of annual streamflow from the control watershed (i.e., wetness conditions). Figure 4 shows the predicted change in postfire annual streamflow, along with the associated standard errors. When the percentage change in annual streamflow was transformed into a volumetric (mm) change, only small increases in postfire annual streamflow were observed during dry years. Postfire annual streamflow response increased with annual wetness conditions until reaching a maximum of 168 mm when annual streamflow from the control watershed was 446 mm, or approximately 6 times mean wetness conditions (Figure 4). When annual streamflow from the control watershed exceeded this threshold, postfire streamflow response began to decrease again.

**Table 5.** Fixed Effect Estimates (Mode) and 95% Credible Intervals for All Models[a]

| Model | Intercept | Control Q | Fire (Uniform) | Fire (Percentage Area Burned) | Fire (Postfire Recovery) | Fire (Percentage Area Burned and Postfire Recovery) | Control Q × Fire (Percentage Area Burned and Postfire Recovery) |
|---|---|---|---|---|---|---|---|
| 1 | 4.54 (3.87/5.07) | | | | | | |
| 2 | 4.31 (3.73/5.01) | 0.81 (0.76/0.86) | | | | | |
| 3 | 4.35 (3.66/5.02) | 0.84 (0.67/1.01) | | | | | |
| 4a | 4.37 (3.61/4.98) | 0.84 (0.66/1.02) | 0.31 (0.18/0.43) | | | | |
| 4b | 4.36 (3.61/4.93) | 0.82 (0.66/1.02) | | 0.42 (0.26/0.57) | | | |
| 4c | 4.33 (3.60/4.97) | 0.83 (0.66/1.02) | | | 0.62 (0.43/0.84) | | |
| 4d | 4.33 (3.64/4.97) | 0.84 (0.66/1.02) | | | | 0.86 (0.61/1.13) | |
| 5 | 4.39 (3.75/5.05) | 0.85 (0.68/1.05) | | | | 0.85 (0.60/1.10) | −0.27 (−0.46/−0.05) |

[a]The variable for Control Q was logged and centered at 4.33.

## 5. Discussion

The results of this study provide strong evidence that despite the variability observed in postfire response at a watershed scale, postfire annual streamflow increases relative to prefire annual streamflow at a regional scale. All four of the fire variables tested in Models 4a–4d had 95% credible intervals that did not overlap with zero (Table 5). The fire variable in Model 4a showed the smallest postfire increase 36% (20%–53%) due to the postfire response being distributed equally over all watersheds and the entire 7 year postfire period. The fire variable in Model 4d, on the other hand, showed a much sharper postfire increase in annual streamflow 136% (84%–208%) since the increase was only applicable to the first postfire year in watersheds that were 100% burned.

The best model in the study (Model 5) included a fire variable that incorporated both the postfire recovery of vegetation and the percentage of watershed burned. For the former component, the effect of fire on streamflow was best represented by the normalized postfire vegetation recovery curve, which was better able to capture postfire streamflow response in these watersheds than a dummy variable approach. The effect of fire was most pronounced during the first postfire year when reductions in vegetation were greatest, then decreased over a 7 year period as vegetation communities became reestablished. These results suggest that at a regional scale, postfire reductions in shrubland and other vegetation types present in the watersheds have a larger effect on postfire ET than corresponding increases in herbaceous vegetation.

Percentage of watershed area burned was shown to be an important control on postfire streamflow change at the regional level. For average annual wetness conditions, postfire annual streamflow increased 134%, or 102 mm, during the first postfire year assuming 100% area burned (Model 5). This regional increase is similar to the results obtained by *Bosch and Hewlett* [1982] who found that annual streamflow increased ~10 mm for every 10% decrease in scrub cover. The similarity of results between the two studies suggests that annual streamflow response to land-cover change at regional scales may not be as variable as response at watershed scales.

Annual streamflow response to fire was lowest during dry years, greatest during wet years, and then slowly decreased for extremely wet years (Figure 4). A possible physical explanation for these results relates to the interaction between soil drainage and rooting depth [*Wilcox et al.*, 2006]. During dry years, the storage capacity within the shallow rooting zone of the herbaceous vegetation that dominate early postfire succession may be sufficient to transpire all available soil water, minimizing the transpirational differences

**Table 6.** Random Effect Estimates (Mode) and 95% Credible Intervals for All Models

| Model | Level-2 Variance (Intercept) | Level-2 Variance (Slope) | Level-2 Covariance (Intercept and Slope) | Level-1 Variance (Residual) |
|---|---|---|---|---|
| 1 | 0.66 (0.28/2.12) | | | 1.44 (1.20/1.70) |
| 2 | 0.90 (0.37/2.39) | | | 0.29 (0.25/0.36) |
| 3 | 0.97 (0.38/2.85) | 0.05 (0.02/0.18) | −0.14 (−0.56/0.006) | 0.22 (0.18/0.25) |
| 4a | 0.96 (0.41/2.94) | 0.07 (0.02/0.19) | −0.17 (−0.57/0.009) | 0.20 (0.16/0.23) |
| 4b | 0.94 (0.40/2.85) | 0.06 (0.02/0.19) | −0.14 (−0.57/0.004) | 0.19 (0.16/0.23) |
| 4c | 0.89 (0.39/2.90) | 0.06 (0.02/0.19) | −0.15 (−0.58/0.001) | 0.18 (0.15/0.22) |
| 4d | 0.87 (0.38/2.81) | 0.06 (0.02/0.20) | −0.15 (−0.58/0.003) | 0.18 (0.15/0.22) |
| 5 | 0.89 (0.39/2.87) | 0.06 (0.02/0.20) | −0.14 (−0.56/0.011) | 0.17 (0.15/0.21) |

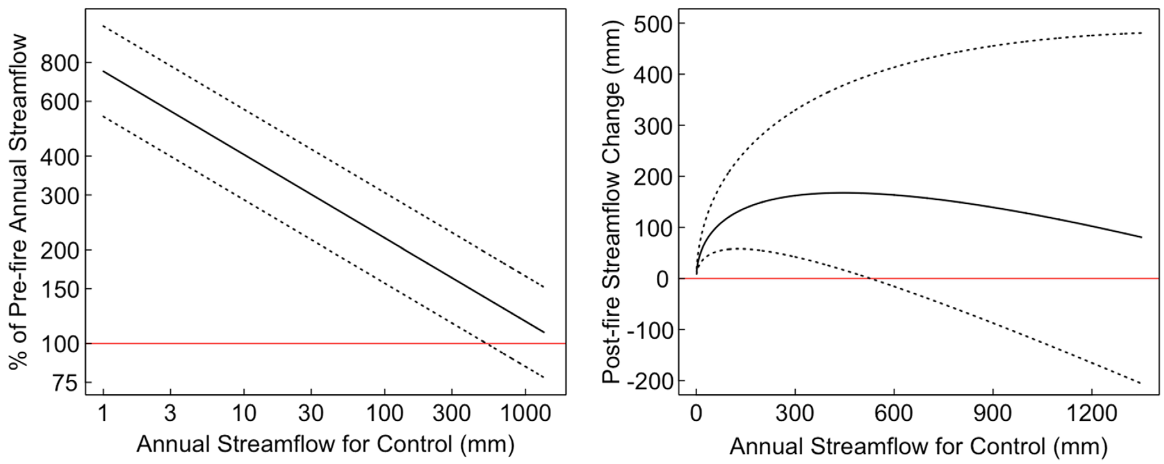


**Figure 4.** Predicted change (% and mm) in annual flow during the first postfire year, adjusted for annual wetness conditions. Dashed lines represent standard errors for the prediction.

between postfire herbaceous vegetation and prefire chaparral and trees. During years with higher levels of wetness, the effect of differences in prefire and postfire rooting depth on vegetation transpiration becomes more pronounced. Water that may be available for transpiration by shrubs and trees under prefire conditions moves beyond the rooting zone of herbaceous vegetation under postfire conditions. This difference in water availability for transpiration increases the likelihood that postfire annual streamflow will increase at higher wetness levels relative to lower levels. A similar effect has been noted by *Zhang et al*. [2001], who observed that the effect of vegetation rooting depth on mean annual transpiration was greatest for intermediate wetness conditions. This result also supports observations made by *Bart and Hope* [2010] and *Feikema et al*. [2013] that increases in annual wetness enhance postfire streamflow change. For extremely wet years, transpiration becomes slightly less sensitive to differences in prefire and postfire rooting depths as precipitation frequency becomes sufficient to sustain transpiration at potential levels for both pre- and postfire vegetation.

The mixed modeling approach used in this study appears to be a viable technique for modeling postfire changes in annual streamflow at a regional scale. Still, the findings should be evaluated in the context of the assumptions and uncertainty of the modeling approach. The mixed model assumed that the watersheds used in calibration were a random sample taken from a larger population of watersheds. The watersheds in this study did not satisfy this assumption and were instead selected based on available USGS gauged watersheds meeting preestablished criteria. The effect of this bias in sampling on model inference is unclear.

Perhaps more significant is the limitation of using only 12 watershed pairs to estimate a regional-level response. The 12 paired watersheds in this study were the only pairs within central and southern California that satisfied the selection criteria. Watersheds in this region are subject to frequent fires, making it challenging to identify burned and control watersheds with fire-free periods that are sufficient to establish a calibration relation [*Bart and Hope*, 2010]. The small number of watersheds contributed to large uncertainty associated with the regional estimates of postfire annual streamflow (e.g., 82%–200% for Model 5). Nonetheless, predictions of postfire streamflow change based on the regional estimates are likely to have less uncertainty and represent an improvement over predictions based on individual watershed experiments.

An increase in the number of paired watersheds would not only reduce uncertainty in the results, but would also allow the effects of watershed characteristics (e.g., watershed area, soil depth, etc.) on postfire streamflow change to be examined. For example, many of the burned watersheds with large postfire increases in streamflow (Figure 3) are located in smaller watersheds (Table 1). However, there are confounding issues with establishing a relation between watershed area and postfire streamflow change because many of the larger watersheds that show little postfire streamflow change were subject to postfire droughts. In addition, the larger watersheds are geographically clustered in the northern part of the study area, which could also indicate subregional differences in postfire streamflow response. The mixed model may be used to tease apart these confounding factors to identify watershed-level controls on postfire streamflow change. Unfortunately, the complexity of the mixed model when incorporating watershed-level variables was not supported by the data available in this study.

Finally, the use of remote sensing could be used to potentially improve the regional estimate of postfire annual streamflow response. A single vegetation response curve was used in this study to represent vegetation recovery for all watersheds. However, for fires occurring within the satellite era, direct quantification of the postfire recovery in each watershed may better characterize postfire hydrologic response, as vegetation recovery may vary depending by species distribution and postfire meteorological conditions [*Hope et al.*, 2012]. Further, while this study used fire perimeters to quantify levels of postfire vegetation change, incorporation of remotely sensed burn severity metrics, such as the differenced Normalized Burn Ratio [*Miller and Thode*, 2007], may also decrease the uncertainty of the results.

## 6. Conclusions

Previous investigations into the effect of fire on annual streamflow have shown that while postfire streamflow often increases, the effect may be quite variable from watershed to watershed. For this study, the regional effect of fire on annual streamflow was estimated for watersheds in central and southern California. Using a mixed modeling approach, the best model for predicting postfire streamflow change included a fire variable that accounted for both differences in percentage area burned and postfire vegetation recovery, as well as an interaction variable describing the influence of annual wetness conditions.

At a regional scale, postfire annual streamflow was predicted to increase 134% (82%–200%) during the first postfire year assuming 100% area burned and average annual wetness conditions. Postfire response decreased with lower percentages of watershed area burned and during subsequent years as vegetation recovered following fire. Regional response also varied interannually based on annual wetness conditions, with the effect of fire being smallest during dry years, greatest during wet years, and slowly decreasing during very wet years. These findings provide watershed managers with a first-order estimate for predicting postfire streamflow response in both gauged and ungauged watersheds. The results may also be used for modeling the effects of climate change and changes in fire regimes on streamflow.

**Acknowledgments**
Data used for the analysis are available as supporting information Table S1. I am indebted to Allen Hope, who selflessly assisted me in many aspects of this paper. I am also very grateful for the comments and feedback provided by Christina (Naomi) Tague, Oliver Chadwick, Trent Biggs, and each of reviewers.

## References

Aronica, G., A. Candela, and M. Santoro (2002), Changes in the hydrological response of two Sicilian basins affected by fire, in *FRIEND 2002-Regional Hydrology: Bridging the Gap Between Research and Practice*, edited by H. A. J. van Lanen and S. Demuth, pp. 163–169, IAHS Press, Wallingford, U. K.

Bart, R., and A. Hope (2010), Streamflow response to fire in large catchments of a Mediterranean-climate region using paired-catchment experiments, *J. Hydrol.*, *388*, 370–378, doi:10.1016/j.jhydrol.2010.05.016.

Bickel, R. (2007), *Multilevel Analysis for Applied Research: It's Just Regression!*, The Guilford Press, N. Y.

Bosch, J. M., and J. D. Hewlett (1982), A review of catchment experiments to determine the effect of vegetation changes on water yield and evapotranspiration, *J. Hydrol.*, *55*(1–4), 3–23, doi:10.1016/0022-1694(82)90117-2.

Britton, D. L. (1991), Fire and the chemistry of a South African mountain stream, *Hydrobiologia*, *218*(3), 177–192, doi:10.1007/BF00038834.

Brown, A. E., L. Zhang, T. A. McMahon, A. W. Western, and R. A. Vertessy (2005), A review of paired catchment studies for determining changes in water yield resulting from alterations in vegetation, *J. Hydrol.*, *310*(1–4), 28–61, doi:10.1016/j.jhydrol.2004.12.010.

Callaway, R. M., and F. W. Davis (1993), Vegetation dynamics, fire, and the physical environment in coastal central California, *Ecology*, *74*(5), 1567–1578, doi:10.2307/1940084.

Chamizo, S., Y. Cantón, R. Lázaro, and F. Domingo (2013), The role of biological soil crusts in soil moisture dynamics in two semiarid ecosystems with contrasting soil textures, *J. Hydrol.*, *489*, 74–84, doi:10.1016/j.jhydrol.2013.02.051.

Clarke, R. T. (2001), Separation of year and site effects by generalized linear models in regionalization of annual floods, *Water Resour. Res.*, *37*(4), 979–986, doi:10.1029/2000WR900370.

Enders, C. K., and D. Tofighi (2007), Centering predictor variables in cross-sectional multilevel models: A new look at an old issue, *Psychol. Methods*, *12*(2), 121–138, doi:10.1037/1082-989X.12.2.121.

Falcone, J. A. (2011), *GAGES-II: Geospatial attributes of gages for evaluating streamflow*, U.S. Geological Survey, Reston, Va. [Available at http://water.usgs.gov/GIS/metadata/usgswrd/XML/gagesII_Sept2011.xml, accessed on September 3, 2013.]

Feikema, P. M., C. B. Sherwin, and P. N. J. Lane (2013), Influence of climate, fire severity and forest mortality on predictions of long term streamflow: Potential effect of the 2009 wildfire on Melbourne's water supply catchments, *J. Hydrol.*, *488*, 1–16, doi:10.1016/j.jhydrol.2013.02.001.

Hadfield, J. D. (2010), MCMC methods for multi-response generalized linear mixed models: The MCMCglmm R package, *J. Stat. Software*, *33*(2), 1–22.

Hope, A., C. Tague, and R. Clark (2007), Characterizing post-fire vegetation recovery of California chaparral using TM/ETM+ time-series data, *Int. J. Remote Sens.*, *28*(6), 1339–1354, doi:10.1080/01431160600908924.

Hope, A., N. Albers, and R. Bart (2012), Characterizing post-fire recovery of fynbos vegetation in the Western Cape Region of South Africa using MODIS data, *Int. J. Remote Sens.*, *33*(4), 979–999, doi:10.1080/01431161.2010.543184.

Hox, J. (2002), *Multilevel Analysis: Techniques and Applications*, Lawrence Erlbaum Assoc., Mahwah, N. J.

Hoyt, W. G., and H. C. Troxell (1932), Forests and stream flow, *Proc. Am. Soc. Civ. Eng.*, *58*, 1037–1066.

Jung, H. Y., T. S. Hogue, L. K. Rademacher, and T. Meixner (2009), Impact of wildfire on source water contributions in Devil Creek, CA: Evidence from end-member mixing analysis, *Hydrol. Processes*, *23*(2), 183–200, doi:10.1002/hyp.7132.

Keeley, J. E., and C. J. Fotheringham (2003), Impact of past, present, and future fire regimes on North American Mediterranean shrublands, in *Fire and Climatic Change in Temperate Ecosystems of the Western Americas*, edited by T. T. Veblen et al., pp. 218–262, Springer, N. Y.

Keeley, J. E., and S. C. Keeley (1981), Post-fire regeneration of southern California chaparral, *Am. J. Bot.*, *68*(4), 524–530.

Keller, E. A., D. W. Valentine, and D. R. Gibbs (1997), Hydrological response of small watersheds following the Southern California Painted Cave Fire of June 1990, *Hydrol. Processes*, *11*(4), 401–414, doi:10.1002/(SICI)1099-1085(19970330)11:4<401::AID-HYP447>3.0.CO;2-P.

Kinoshita, A. M., and T. S. Hogue (2011), Spatial and temporal controls on post-fire hydrologic recovery in Southern California watersheds, *Catena*, *87*(2), 240–252, doi:10.1016/j.catena.2011.06.005.

Kohavi, R. (1995), A study of cross-validation and bootstrap for accuracy estimation and model selection, in *International Joint Conference on Artificial Intelligence*, vol. 14, pp. 1137–1145, Morgan Kaufmann, San Francisco, Calif.

Lavabre, J., S. Torres, and F. Cernesson (1993), Changes in the hydrological response of a small Mediterranean basin a year after a wildfire, *J. Hydrol.*, *142*(1), 273–299, doi:10.1016/0022-1694(93)90014-Z.

Lenihan, J. M., R. Drapek, D. Bachelet, and R. P. Neilson (2003), Climate change effects on vegetation distribution, carbon, and fire in California, *Ecol. Appl.*, *13*(6), 1667–1681, doi:10.1890/025295.

Lessels, J. S., and T. F. A. Bishop (2013), Estimating water quality using linear mixed models with stream discharge and turbidity, *J. Hydrol.*, *498*, 13–22, doi:10.1016/j.jhydrol.2013.06.006.

Loáiciga, H. A., D. Pedreros, and D. Roberts (2001), Wildfire-streamflow interactions in a chaparral watershed, *Adv. Environ. Res.*, *5*(3), 295–305, doi:10.1016/S1093-0191(00)00064-2.

Lopez-Moreno, J. I., and M. Stähli (2008), Statistical analysis of the snow cover variability in a subalpine watershed: Assessing the role of topography and forest interactions, *J. Hydrol.*, *348*(3), 379–394, doi:10.1016/j.jhydrol.2007.10.018.

McMichael, C. E., and A. S. Hope (2007), Predicting streamflow response to fire-induced landcover change: Implications of parameter uncertainty in the MIKE SHE model, *J. Environ. Manage.*, *84*(3), 245–256, doi:10.1016/j.jenvman.2006.06.003.

McMichael, C. E., A. S. Hope, D. A. Roberts, and M. R. Anaya (2004), Post-fire recovery of leaf area index in California chaparral: A remote sensing-chronosequence approach, *Int. J. Remote Sens.*, *25*(21), 4743–4760, doi:10.1080/01431160410001726067.

Miller, J. D., and A. E. Thode (2007), Quantifying burn severity in a heterogeneous landscape with a relative version of the delta Normalized Burn Ratio (dNBR), *Remote Sens. Environ.*, *109*(1), 66–80, doi:10.1016/j.rse.2006.12.006.

Miller, P. C., D. K. Poole, and P. M. Miller (1983), The influence of annual precipitation, topography, and vegetative cover on soil moisture and summer drought in Southern California, *Oecologia*, *56*(2), 385–391, doi:10.1007/BF00379717.

Moody, J. A., and D. A. Martin (2009), Synthesis of sediment yields after wildland fire in different rainfall regimes in the western United States, *Int. J. Wildland Fire*, *18*(1), 96–115.

Nolan, R. H., P. N. Lane, R. G. Benyon, R. A. Bradstock, and P. J. Mitchell (2015), Trends in evapotranspiration and streamflow following wildfire in resprouting eucalypt forests, *J. Hydrol.*, *524*, 614–624.

Plummer, M. (2008), Penalized loss functions for Bayesian model comparison, *Biostatistics*, *9*(3), 523–539, doi:10.1093/biostatistics/kxm049.

Ryan, T. P. (1997), *Modern Regression Methods*, John Wiley, N. Y.

Scott, D. F. (1993), The hydrological effects of fire in South African mountain catchments, *J. Hydrol.*, *150*(2), 409–432, doi:10.1016/0022-1694(93)90119-T.

Seo, J. I., F. Nakamura, D. Nakano, H. Ichiyanagi, and K. W. Chun (2008), Factors controlling the fluvial export of large woody debris, and its contribution to organic carbon budgets at watershed scales, *Water Resour. Res.*, *44*, W04428, doi:10.1029/2007WR006453.

Shakesby, R. A., and S. H. Doerr (2006), Wildfire as a hydrological and geomorphological agent, *Earth Sci. Rev.*, *74*(3–4), 269–307, doi:10.1016/j.earscirev.2005.10.006.

Smith, H. G., G. J. Sheridan, P. N. Lane, P. Nyman, and S. Haydon (2011), Wildfire effects on water quality in forest catchments: A review with implications for water supply, *J. Hydrol.*, *396*(1), 170–192.

Spiegelhalter, D. J., N. G. Best, B. P. Carlin, and A. van der Linde (2002), Bayesian measures of model complexity and fit, *J. R. Stat. Soc., Ser. B*, *64*(4), 583–639, doi:10.2307/3088806.

Stegmueller, D. (2013), How many countries for multilevel modeling? A comparison of frequentist and Bayesian approaches, *Am. J. Polit. Sci.*, *57*(3), 748–761, doi:10.1111/ajps.12001.

Walsh, C. J., and J. A. Webb (2014), Spatial weighting of land use and temporal weighting of antecedent discharge improves prediction of stream condition, *Landscape Ecol.*, *29*(7), 1171–1185, doi:10.1007/s10980-014-0050-y.

Webb, A. A., and A. Kathuria (2012), Response of streamflow to afforestation and thinning at Red Hill, Murray Darling Basin, Australia, *J. Hydrol.*, *412–413*, 133–140, doi:10.1016/j.jhydrol.2011.05.033.

Wehrly, K. E., T. O. Brenden, and L. Wang (2009), A comparison of statistical approaches for predicting stream temperatures across heterogeneous landscapes, *J. Am. Water Resour. Assoc.*, *45*(4), 986–997, doi:10.1111/j.1752-1688.2009.00341.x.

Westerling, A. L., and B. P. Bryant (2008), Climate change and wildfire in California, *Clim. Change*, *87*(1), 231–249, doi:10.1007/s10584-007-9363-z.

Wilcox, B. P., M. K. Owens, W. A. Dugas, D. N. Ueckert, and C. R. Hart (2006), Shrubs, streamflow, and the paradox of scale, *Hydrol. Processes*, *20*(15), 3245–3259, doi:10.1002/hyp.6330.

Williams, A. A. J., D. J. Karoly, and N. Tapper (2001), The sensitivity of Australian fire danger to climate change, *Clim. Change*, *49*(1), 171–191, doi:10.1023/A:1010706116176.

Zhang, L., W. R. Dawes, and G. R. Walker (2001), Response of mean annual evapotranspiration to vegetation changes at catchment scale, *Water Resour. Res.*, *37*(3), 701–708, doi:10.1029/2000WR900325.